

# Perfect Scalars on the Lattice

W. Bietenholz

NORDITA  
Blegdamsvej 17  
DK-2100 Copenhagen Ø, Denmark

Preprint NORDITA-1999/69-HE

We perform renormalization group transformations to construct optimally local perfect lattice actions for free scalar fields of any mass. Their couplings decay exponentially. The spectrum is identical to the continuum spectrum, while thermodynamic quantities have tiny lattice artifacts. To make such actions applicable in simulations, we truncate the couplings to a unit hypercube and observe that spectrum and thermodynamics are still drastically improved compared to the standard lattice action. We show how preconditioning techniques can be applied successfully to this type of action. We also consider a number of variants of the perfect lattice action, such as the use of an anisotropic or triangular lattice, and modifications of the renormalization group transformations motivated by wavelets. Along the way we illuminate the consistent treatment of gauge fields, and we find a new fermionic fixed point action with attractive properties.

# 1 Introduction

*Renormalization group transformations* (RGTs) are an important operation, both, in field theory and in statistical mechanics. They allow to vary the cutoff of a system without altering its physical contents. In particular RGT fixed points and their vicinity are of interest, both, conceptually and for practical purposes.

If a system is defined on a (Euclidean) lattice, then RGTs can be performed by block variable transformations and a subsequent rescaling [1]. In particular for the simple system of a free scalar field, it has been shown a long time ago that such block variable RGTs – for instance with blocking factor 2 – can be iterated an infinite number of times in momentum space [2]. For suitably chosen RGT parameters and massless scalars, one arrives at a finite *fixed point action* (FPA). There the observables are independent of the lattice spacing – which is an inverse UV cutoff – so that we can represent exact continuum physics on the lattice.

In each transformation step the average of the variables in one block of the fine lattice is related to the corresponding block variable on the coarse lattice. This has often been implemented by a  $\delta$  function. However, the  $\delta$  function is just one possibility in a class of implementations, which keep the partition function and all expectation values invariant. In Ref. [2] a generalization was suggested, where this relation is smoothly implemented by a Gaussian, and it was observed that in this way the locality of the FPA can be improved.

<sup>1</sup> This is very important for practical purposes, because one ultimately has to truncate the couplings to short distances, and to hope that this truncation does not affect the perfect properties too much. If one sends the blocking factor to infinity, then one single RGT leads to the FPA [3, 4]. This amounts to a technique that we call “blocking from the continuum”: one starts from a continuum theory and defines lattice variables by relating each of them to the Riemann integral over a lattice cell.

A similar construction has been realized for free fermions with a  $\delta$  function RGT [5] and a generalized RGT [6]. In that context the FPA also yielded new insight into the fermion doubling problem. By a somewhat more complicated RGT one obtains a FPA for staggered fermions too [7]. Also here we can optimize locality by using a smooth RGT [8] and the result can be reproduced again by blocking from the continuum [9, 10]. Moreover, blocking from the continuum also leads to a fixed point for free non-compact gauge fields [11].

FPA have the remarkable property that a system is regularised but not contaminated by any cutoff artifacts. Of course it is a dream to construct such a regularisation also for interacting theories at arbitrary correlation length  $\xi$  (FPAs only exist at  $\xi = \infty$ ). Indeed, general arguments show that such “*perfect lattice actions*” do exist even at finite correlation length [1], but they are hard to construct. By blocking from the continuum this can be achieved at least perturbatively, and the perfect action was constructed explicitly to first order in the fermion-gauge coupling for the Schwinger model [4] and for QCD

---

<sup>1</sup>Also the scalar FPA of the  $\delta$  function RGT is local in the sense of an exponential decay of the couplings (in contrast to the fermionic FPA), but for certain Gaussian RGTs this decay becomes even faster, see Section 2.

[11, 12, 13]. For the anharmonic oscillator, the first order perturbatively perfect action has been constructed and simulated in order to test its scaling and asymptotic scaling behavior [14].

This approach to fight artifacts due to the finite lattice spacing – which are the worst systematic errors in many Monte Carlo simulations – has picked up new momentum since the appearance of Ref. [15]. There the authors noticed that for asymptotically free theories the construction of a FPA (with rescaling of the weakly relevant coupling) is a classical field theory problem.<sup>2</sup> Hence it can be solved by minimization instead of (numerical) functional integrals, which simplifies the task enormously. Moreover the authors suggest to use the FPA, which is a classically perfect action, even at moderate correlation length, and they demonstrated for the 2d  $O(3)$  model that this can be a very successful approximation of a perfect lattice action. The construction can be performed non-perturbatively, by numerical inverse blocking RGTs. Of course for complicated theories like QCD, or pure  $SU(3)$  gauge theory [17], even this approximation is tedious. In addition, problems related to the parameterization and truncation of such quasi-perfect actions are difficult to handle, but crucial for potential applications. With this respect it is advisable to start from a simple situation and study there, which procedures are promising. The present paper is a contribution to that issue. A synopsis of our results was anticipated in Ref. [18].

In this paper we deal with scalar fields. In analogy to the previously studied fermions, the free particles provide an improved formulation, which is promising also in the presence of interactions. In Section 2 we derive perfect lattice actions for free lattice fields by blocking from the continuum and we optimize their locality. In Section 3 we truncate the couplings to a unit hypercube and consider the effect on the dispersion relation. In Section 4 we illustrate the improved thermodynamic scaling properties of this “*hypercube scalar*”. For the evaluation of the scalar matrix – analogous to the fermion matrix – we can still use preconditioning in the hypercubic case, as we show in Section 5. In Section 6 we discuss perfect actions on anisotropic and triangular lattices. As a further alternative we consider in Section 7 a class of new blocking prescriptions, which is motivated by the wavelet resp. B-spline formalism. The most promising new variant is also applied to fermions (Appendix B). Section 8 contains our conclusions and an outlook on applications.

## 2 Perfect lattice scalar actions

Let us start from a scalar field  $\phi$  and its action  $S[\phi]$  on a hypercubic lattice in  $d$  dimensional Euclidean space. The Kadanoff transformation to a coarser lattice can be written as [19]

$$e^{-S'[\phi']} = \int \mathcal{D}\phi \, K[\phi', \phi] e^{-S[\phi]} \quad (2.1)$$

---

<sup>2</sup>Alternatively there are many attempts to use real space blocking RGTs (without classical approximation). For recent work on scalars resp. pure  $SU(3)$  gauge fields, see Ref. [16]. A limitation there is that one can hardly implement the blocking constraint in a way different from the  $\delta$  function.

where  $S'[\phi']$  is the action of the new scalar field  $\phi'$  on the coarse lattice. We integrate over the lattice measure  $\mathcal{D}\phi = \int \prod_x d\phi_x$ . The kernel  $K[\phi', \phi]$  has to be chosen such that the partition function and its derivatives remain invariant under this transformation (up to a possible constant factor). This can be achieved by the requirement

$$\int \mathcal{D}\phi' K[\phi', \phi] = \text{const.} \quad (2.2)$$

The simplest and most popular choice is

$$K[\phi', \phi] = \prod_{x'} \delta(\phi'_{x'} - A_{x'}[\phi]). \quad (2.3)$$

Here  $x'$  runs over the coarse lattice, and the symbol  $A_{x'}[\phi]$  is an average taken in the block of the fine lattice, which is attached to  $x'$ . For instance, one may just take the arithmetic mean value together with a rescaling factor,

$$A_{x'}[\phi] = \frac{b_n}{n^d} \sum_{x \in x'} \phi_x. \quad (2.4)$$

This sum extends over all the  $n^d$  fine lattice points in the block associated with  $x'$ . After the transformation we express all quantities in units of the coarse lattice. The factor  $b_n$  is used to neutralize this rescaling so that we can arrive at a finite FPA. Hence its value is determined by the dimension of the scalar field,

$$b_n = n^{(d-2)/2}. \quad (2.5)$$

However, the choice (2.3) is by no means unique. A class of generalizations has been considered by Bell and Wilson, where the  $\delta$  function is replaced by a Gaussian [2],

$$K[\phi', \phi] = \exp \left\{ -\frac{2}{\alpha} \sum_{x'} [\phi'_{x'} - A_{x'}[\phi]]^2 \right\}, \quad (\alpha \geq 0). \quad (2.6)$$

In the limit  $\alpha \rightarrow 0$  we return to the  $\delta$  RGT (2.3), but the condition (2.2) holds for all positive  $\alpha$ .

In Ref. [2] the fixed point for a massless scalar particle has been computed by an infinite number of iterations of such block factor 2 RGTs. The iteration starts from the standard lattice action in momentum space,

$$S[\phi] = \frac{1}{(2\pi)^d} \int d^d k \, \phi(-k) \frac{1}{2} \hat{k}^2 \phi(k), \quad (\hat{k}_\mu := 2 \sin \frac{k_\mu}{2}), \quad (2.7)$$

where we set the lattice spacing equal to 1.

However, instead of this tedious iteration we can also send the blocking factor  $n \rightarrow \infty$ , so we obtain a FPA by performing only one RGT [3, 4]. Since we call the spacing of the final lattice 1 again, the original lattice variables move closer and closer together (in

the final units) as  $n$  increases. Finally the sum in condition (2.2) turns into a Riemann integral,

$$A_x \varphi = \int_{C_x} d^d y \varphi(y). \quad (2.8)$$

Here we do not start from a field  $\phi_x$  on a fine lattice any longer, but from a continuum field  $\varphi(y)$ . We integrate over hypercubic unit cells  $C_x$  with centers  $x$ , and relate those integrals to the new lattice variables  $\phi_x$ . Also the action on the fine lattice is replaced by the continuum action. Now the RGT step requires a continuum path integral, so it can only be computed in certain cases. Of course this limit  $n \rightarrow \infty$  can also be taken for the generalized form (2.6).

We first reproduce this calculation in its short-cut form, including also an arbitrary mass  $m$  of the scalar field. There is no FPA at  $m > 0$ , but we construct an entire renormalized trajectory, i.e. a curve of perfect lattice actions, for free scalars of any mass. It is parameterized by  $m$  and crosses the critical surface in a fixed point at  $m = 0$ .

The lattice action is given by

$$\begin{aligned} e^{-S[\phi]} = & \int \mathcal{D}\phi \mathcal{D}\sigma \exp \left\{ -\frac{1}{(2\pi)^d} \int_B d^d k \times \right. \\ & \left[ \frac{1}{2} \sum_{l \in \mathbb{Z}^d} \varphi(-k - 2\pi l) [(k + 2\pi l)^2 + m^2] \varphi(k + 2\pi l) \right. \\ & \left. \left. + i\sigma(-k) [\phi(k) - \sum_{l \in \mathbb{Z}^d} \varphi(k + 2\pi l) \Pi(k + 2\pi l)] + \frac{\alpha}{2} \sigma(-k) \sigma(k) \right] \right\}, \quad (2.9) \end{aligned}$$

where  $B = ]-\pi, \pi]^d$  is the (first) Brillouin zone. We have introduced an auxiliary lattice scalar variable  $\sigma$ , and the function  $\Pi$  is defined as

$$\Pi(k) = \prod_{\mu=1}^d \frac{\hat{k}_\mu}{k_\mu}. \quad (2.10)$$

We can write eq. (2.8) as a convolution,

$$A_x \phi = \int d^d y f(x - y) \varphi(y), \quad f(u) = \begin{cases} 1 & |u_\mu| \leq \frac{1}{2}, \mu = 1, \dots, d \\ 0 & \text{otherwise} \end{cases}, \quad (2.11)$$

and  $\Pi(k)$  is the Fourier transform of  $f(u)$ . Instead of the piece-wise constant function used here one may also insert other functions  $f(u)$ , if they fall off sufficiently fast. Some options will be discussed in Section 7.

We denote the continuum propagator as

$$\Delta(k) := \frac{1}{k^2 + m^2}, \quad (2.12)$$

substitute

$$\tilde{\varphi}(k + 2\pi l) = \varphi(k + 2\pi l) - i\sigma(k) \Delta(k + 2\pi l) \Pi(k + 2\pi l), \quad (2.13)$$

and carry out the Gaussian integration over  $\tilde{\varphi}$ :

$$\begin{aligned} e^{-S[\phi]} &= \int \mathcal{D}\sigma \exp \left\{ \frac{1}{(2\pi)^d} \int_B d^d k [i\sigma(-k)\phi(k) - \frac{1}{2}\sigma(-k)G(k)\sigma(k)] \right\}, \\ G(k) &:= \sum_{l \in \mathbb{Z}^d} \Delta(k + 2\pi l) \Pi^2(k + 2\pi l) + \alpha. \end{aligned} \quad (2.14)$$

By further substituting

$$\tilde{\sigma}(k) = \sigma(k) - iG(k)^{-1}\phi(k) \quad (2.15)$$

and integrating  $\tilde{\sigma}$  we arrive at

$$S[\phi] = \frac{1}{(2\pi)^d} \int_B d^d k \frac{1}{2} \phi(-k) G(k)^{-1} \phi(k), \quad (2.16)$$

which shows that  $G(k)$  is the perfect free lattice propagator. Note that this scalar perfect lattice action is also the renormalized trajectory of the  $O(N)$  non-linear  $\sigma$  model in the limit  $N \rightarrow \infty$  (up to a factor  $N$ ) [20, 21], in analogy to the large  $N$  limit of the Gross Neveu model [22]. The sum over  $l \in \mathbb{Z}^d$  converges in any dimension thanks to the  $\Pi$  function, but it can be computed analytically only in  $d = 1$ . If we now specify the RGT “smearing parameter” (because it smears the  $\delta$  function to a Gaussian) to be

$$\alpha = \bar{\alpha}(m) := \frac{\sinh m - m}{m^3}, \quad (2.17)$$

then the perfect action in  $d = 1$  becomes ultralocal,

$$G_{d=1}(k) = \frac{\sinh m \cdot \hat{m}^2}{m^3} \frac{1}{\hat{k}^2 + \hat{m}^2}, \quad \hat{m} := 2 \sinh \frac{m}{2}. \quad (2.18)$$

In this case, the couplings are even restricted to nearest neighbors. In particular the 1d fixed point propagator (defined at  $m = 0$ , where  $\bar{\alpha} = 1/6$ ) is identical to the standard lattice propagator  $1/\hat{k}^2$ . This is obviously the choice for  $\alpha$ , which optimizes the locality in  $d = 1$ . For a general blocking factor  $n$ , the 1d perfect propagator turns ultralocal with

$$\bar{\alpha}_n(m) := \bar{\alpha}(m) \left(1 - \frac{1}{n^2}\right). \quad (2.19)$$

In higher dimensions – that is, in field theory – locality of the perfect propagator can only be achieved in the sense of an exponential decay. For fermions the RGT parameters which provide ultralocality in  $d = 1$  have been used successfully also in higher dimensions. It turned that they still yield extremely local perfect actions in  $d > 1$  [6, 8, 11, 10]. For free gauge fields, a similar (but somewhat more complicated) smearing term leads to ultralocality (the standard plaquette action) in  $d = 2$  and extreme locality in  $d = 4$  [11, 10]. Hence we are guided to apply the same strategy to scalar fields and use  $\alpha = \bar{\alpha}$  as given in eq. (2.17) in any dimension.

Bell and Wilson compared numerically various smearing parameters in  $d = 3$ , and in the fixed point they found optimal locality at  $1/\alpha_2 \simeq 8$ , which agrees with the value resulting from our analytical method.

The perfectness of the action (2.16) can be verified by an explicit additional block factor  $n$  transformation ( $n < \infty$ ). This is demonstrated in Appendix A. The result is that a block factor  $n$  RGT applied on  $G(k)$  at mass  $m$  reproduces  $G(k)$ , now at mass  $n \cdot m$ . This is exactly the expected behavior on the renormalized trajectory. This calculation also justifies eq. (2.19) as a generalization of  $\bar{\alpha} = \bar{\alpha}_\infty$  given in eq. (2.17).

Let us consider the spectrum of the perfect lattice action (2.16). We denote  $k = (\vec{k}, k_d)$  and identify the energy as  $E = i(k_d + 2\pi l_d)$ . Thus the spectrum is given by

$$E^2 = (\vec{k} + 2\pi \vec{l})^2 + m^2. \quad (2.20)$$

There is a branch for each  $\vec{l}$ . The branch for  $\vec{l} = \vec{0}$  is the *exact* continuum spectrum. In this sense, the full, continuous Poincaré invariance is present in the perfect lattice action. We emphasize that the form of the lattice action itself does not reveal this property: for instance, the hypercubic structure of the lattice is visible in it, and perfect actions on non hypercubic lattices have different forms, see Section 6 for examples. However, physical observables do have the full continuum symmetries, without any artifacts due to the finite lattice spacing.

The higher branches in the spectrum are required for perfection, since the lattice imposes  $2\pi$  periodicity on the momenta.

We now address the question of *locality*. For massless Wilson-like fermions and a  $\delta$  function RGT one obtains a nonlocal fixed point. Its couplings do not decay exponentially, but only  $\propto r^{1-d}$  [5]. This is the way a contradiction with the Nielsen-Ninomiya theorem is avoided.<sup>3</sup> However, there is no theorem forbidding the scalar  $\delta$  function FPA to be local. We analyze this issue in  $d = 1$ .

A perfect lattice fermion propagator – constructed in analogy to eq. (2.9) – reads [11]

$$G^f(k) = \sum_{l \in \mathbb{Z}^d} \frac{\Pi(k + 2\pi l)^2}{i(\vec{k} + 2\pi \vec{l}) + m} + \alpha_f, \quad (2.21)$$

where  $\alpha_f$  is a smearing parameter analogous to  $\alpha$ . For  $\alpha_f = 0$  and we obtain in one dimension

$$G_{d=1}^f(k)|_{\alpha_f=0} = \frac{1}{m} - \frac{2}{m^2} \left[ \text{ctgh} \frac{m}{2} - i \text{ctg} \frac{k}{2} \right]^{-1}, \quad k \in ]-\pi, \pi]. \quad (2.22)$$

This propagator has a zero – indicating non-locality – at  $k = \pi$ , iff  $m = 0$ .

The corresponding 1d perfect scalar propagator can be written as

$$G_{d=1}(k)|_{\alpha=0} = \frac{1}{2m} \left[ G_{d=1}^f(k)|_{\alpha_f=0} + G_{d=1}^f(-k)|_{\alpha_f=0} \right]. \quad (2.23)$$

---

<sup>3</sup>For any  $\alpha_f > 0$  the fermionic FPA turns local [6], but then the chiral symmetry of the lattice action is explicitly broken, avoiding again a contradiction with the Nielsen-Ninomiya No-Go theorem. However, this only means that the chiral symmetry is not manifest in the lattice action. In physical observables it is still present [23, 24], similar to the Poincaré invariance, which is present in the spectrum, although not manifest in the action.

Here we don't find any zeros; in particular

$$\lim_{m \rightarrow 0} G_{d=1}(\pi)|_{\alpha=0} = \frac{1}{12}. \quad (2.24)$$

This different behavior of the  $\delta$  function FPA for fermions and scalars persists in higher dimensions.

In coordinate space we write the perfect scalar action as

$$S[\phi] = \frac{1}{2} \sum_{x,y \in \mathbb{Z}^d} \phi_x \rho(x-y) \phi_y, \quad (2.25)$$

where  $\rho(r)$  is the inverse propagator, i.e. the (inverse) Fourier transform of  $G(k)^{-1}$ . Fig. 1 shows how the exponential decay coefficient  $c_1$  on an axis depends on the smearing parameter  $\alpha$ ,  $\rho(i, 0, 0, 0) \propto \exp(-c_1(\alpha)i)$ , at  $m = 0$ ,  $m = 2$  and  $m = 4$ .<sup>4</sup>

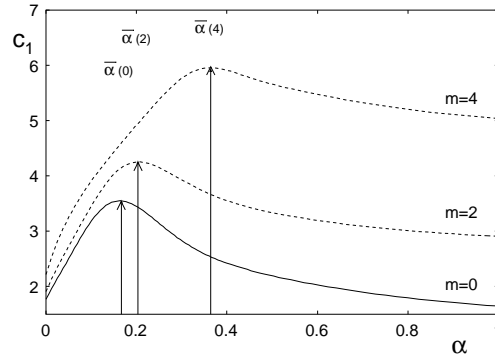


Figure 1: The decay of the couplings  $|\rho(i, 0, 0, 0)| \propto \exp\{-c_1(\alpha)i\}$  of the perfect scalars for masses 0, 2 and 4. The maxima are very close to the values of  $\bar{\alpha}(m)$ , 0.167, 0.203 resp. 0.364, which correspond to eq. (2.17).

The figure confirms that  $\bar{\alpha}$  given in eq. (2.17) is an excellent candidate for optimal locality. It also affirms that the maximum moves to a larger  $\alpha$  as the mass increases. We stay with the neat analytical criterion for the selection of  $\alpha$  presented above, and focus on the mass dependent value of  $\bar{\alpha}$  given in eq. (2.17). Fig. 2 illustrates the exponential decay at various masses. The decay becomes even faster if the mass increases, as it was observed for fermions before [11]. This is illustrated in Fig. 3, where we consider the exponential decay  $|\rho(i, i, i, i)| \propto \exp(-c_4(m)i)$ . Especially in the interval  $m = 0 \dots 2$ , the decay coefficients follow very closely a parabola,

$$c_4(m) \simeq 6.563 + 0.247 m^2. \quad (2.26)$$

The largest couplings in 4d coordinate space for  $m = 0, 1, 2$  and 4 are given in Table 1.

<sup>4</sup>The curves in Fig. 1 are Bezier interpolations, i.e. smooth curves which do not pass through every single data point. Since the exact curve is not that smooth, the Bezier interpolation is appropriate to identify the region of optimal locality.



$r$	$m = 0$	$m = 1$	$m = 2$	$m = 4$
(0000)	4.54276730	4.46018784	4.11732967	2.58349457
(1000)	-0.25656026	-0.21033619	-0.12051159	-0.01815118
(1100)	-0.06722788	-0.05285547	-0.02707061	-0.00294191
(1110)	-0.02211001	-0.01677521	-0.00778413	-0.00061988
(1111)	-0.00828931	-0.00611485	-0.00261666	-0.00015765
(2000)	-0.00079938	-0.00042262	-0.00002726	0.00001090
(2100)	-0.00058401	-0.00036971	-0.00010471	-0.00000201
(2110)	-0.00027747	-0.00018443	-0.00006107	-0.00000192
(2111)	-0.00009663	-0.00006885	-0.00002660	-0.00000098
(2200)	0.00022983	0.00016003	0.00005719	0.00000171
(2210)	0.00013280	0.00008745	0.00002724	0.00000058
(2211)	0.00008482	0.00005317	0.00001456	0.00000022
(2220)	0.00005018	0.00003084	0.00000804	0.00000010
(2221)	0.00003271	0.00001947	0.00000464	0.00000005
(2222)	0.00001011	0.00000573	0.00000120	0.00000001
(3000)	-0.00005999	-0.00003548	-0.00000842	-0.00000009
(3100)	-0.00002060	-0.00001177	-0.00000252	-0.00000002

Table 1: *The largest couplings  $\rho(r)$  of the perfect scalar action in coordinate space for masses  $m = 0, 1, 2$  and  $4$ . The table includes all couplings with absolute values  $\geq 10^{-5}$ .*

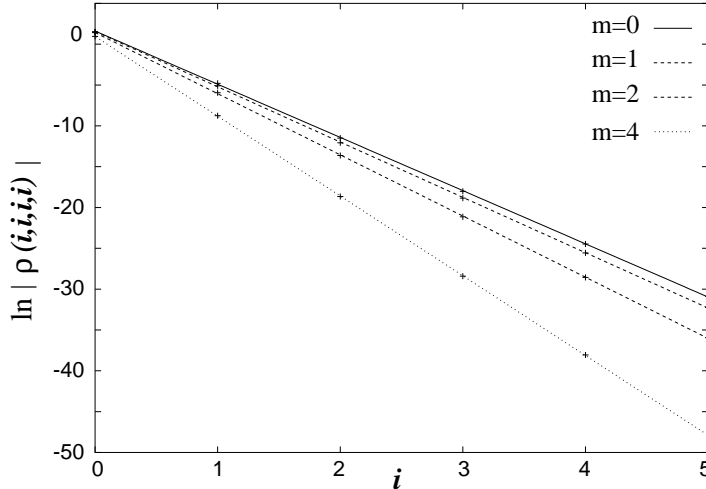


Figure 2: The decay of the couplings  $|\rho(i, i, i, i)|$  in the optimally local perfect scalars for masses 0, 1, 2 and 4. The lines are least square fits to  $|\rho(i, i, i, i)| \propto \exp\{-c_4(m)i\}$ , with  $c_4(0) = 6.515$ ,  $c_4(1) = 6.775$ ,  $c_4(2) = 7.493$  and  $c_4(4) = 9.769$ .

### 3 Truncation by periodic boundary conditions

So far we have worked in an infinite volume, now we consider a hypercubic finite volume with periodic boundary conditions. Of course in a finite volume there are no fixed points in the proper sense, but there are still perfect actions, similar to the perfect actions at finite mass.

Let us fix a volume  $V$  and  $m = 0$ . Then we start from a much larger volume, which shrinks under a number of RGTs (block factor  $< \infty$ ) just to the fixed final volume  $V$ . If we now expand the initial volume more and more, such that the number of RGTs gets larger and larger, then the couplings in  $V$  may converge. Their limit represents the perfect action in the finite volume. (Analogously we can fix a finite ultimate mass in  $V = \infty$  and start from a smaller and smaller initial mass, to obtain after a number of RGTs couplings that converge to those identified for the final mass in Section 2.)

The transition from infinite to finite volume is technically easy: we just replace the integrals over the Brillouin zone in all the formulae of Section 2 by discrete sums, and the rest remains unaltered, including the smearing parameter for optimal locality. We may call this a “decimation in momentum space”. Of course, the couplings  $\rho(r)$  will change a little compared to  $V = \infty$ ; for instance an exponential decay is not possible any more. At the boundary of  $V$  they have to vanish smoothly, which suggests the use of this mechanism as a truncation scheme: we impose periodic boundary conditions in some volume, set the couplings to points outside this volume to zero, and finally use this set of couplings in any volume.

This scheme has a number of virtues: the normalization conditions for  $\sum_r \rho(r)$  and

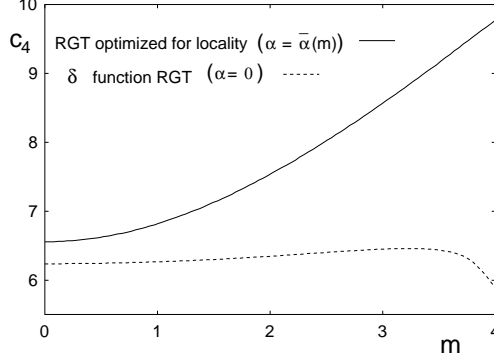


Figure 3: *The decay of the couplings of the perfect scalars – measured by  $c_4$  in  $|\rho(i, i, i, i)| \propto \exp\{-c_4 i\}$  – as a function of the mass  $m$ . The optimally local perfect scalars follow approximately a parabola, and its decay is clearly faster the one obtained from a  $\delta$  function RGT.*

$\sum_r r^2 \rho(r)$  are precisely fulfilled (in particular for  $m = 0$  these sums are 0 resp.  $-2d$ ), and the transitions to lower dimensions by summing over the lattice sites in the supplementary directions is also exact. Hence the selection criterion for the RGT parameters, which refers to the mapping on  $d = 1$ , is still sensible for the truncated system.

All these properties are not obeyed if we truncate by just chopping off the couplings in infinite coordinate space outside a given volume. If we start in this way, we have to re-adjust the normalizations a posteriori, which is quite ambiguous. Moreover, the periodic truncation has a huge practical advantage: certain quantities in perfect lattice perturbation theory take a rather complicated form, such as the perfect quark-gluon vertex in QCD [11, 12]. It is a difficult numerical task to evaluate them and to transform them to coordinate space, where they are ultimately needed. If only a few discrete momenta are involved, this task simplifies tremendously.

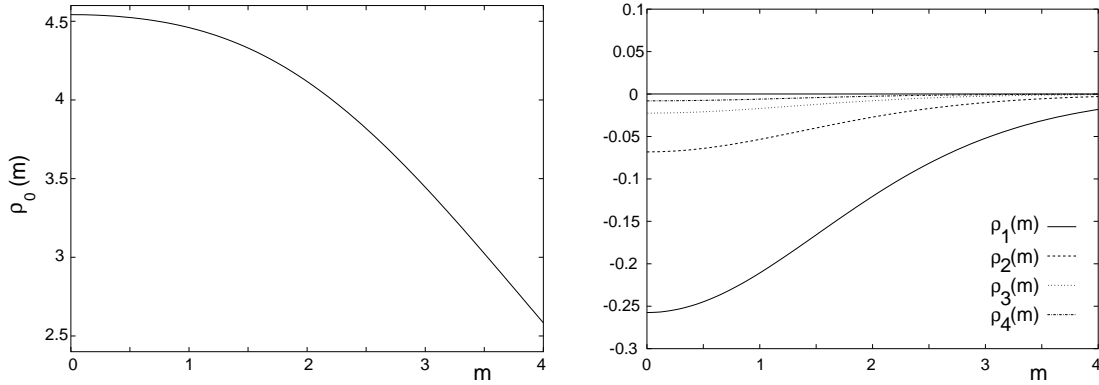


Figure 4: *The mass dependence of the hypercubic couplings  $\rho_0 = \rho(0, 0, 0, 0)$  (left), as well as  $\rho_1 = \rho(1, 0, 0, 0)$ ,  $\rho_2 = \rho(1, 1, 0, 0)$ ,  $\rho_3 = \rho(1, 1, 1, 0)$  and  $\rho_4 = \rho(1, 1, 1, 1)$  (right).*

We apply the preferred procedure by imposing periodic boundary conditions over a distance of 3 lattice spacings. Thus the remaining couplings are restricted to a unit hypercube. There are formally  $3^d$  of them, but they come in just  $d+1$  equivalence classes. Furthermore the mapping condition on the ultralocal 1d case and  $\sum_r r^2 \rho(r)$  impose three constraints on the equivalence classes, such that e.g. in  $d=4$  there remain only two degrees of freedom. We give the full set of  $d+1$  couplings in  $d=2, 3$  and  $4$  for masses  $m=0, 1, 2$  and  $4$  in Table 2, and we illustrate the smooth mass dependence of the truncated 4d couplings in Fig. 4. This truncation range is of practical interest, since it has been shown that hypercube particles are tractable in 4d simulations [13, 25, 26].

One may argue that the really perfect actions of Section 2 (in  $d > 1$ ) are academic, since we always need some truncation for practical purposes. As a first check on how much the perfect properties suffer from the 3-periodic truncation, we show the dispersion relation of the “hypercube scalar” for  $m=0$  and  $m=2$  in Fig. 5, where they are compared to the perfect or continuum spectrum and to the spectrum obtained from the standard lattice action. As an example, we consider the direction (110) and we observe a dramatic improvement, all the way up to the edge of the Brillouin zone. The situation is similar in the (100) and the (111) direction. This is a success of the optimized locality in Section 2. Note that the truncated perfect energies start with a slight overshoot at small momenta. Following Symanzik’s improvement program – which is fundamentally different from the program discussed here – it would be possible to correct the leading order artifacts  $\propto \vec{k}^2$ . Then the dispersion becomes even better for small momenta, but with respect to larger momenta this is not necessarily an advantage. At the edge of the Brillouin zone the curve has to bend down due to periodicity, so it can be favorable to start with a slight overshoot, in order to follow the perfect curve over a wide range. After all, if one wants to simulate on very coarse lattices, then not only the momenta  $|\vec{k}| \ll 1$  are important. We also emphasize that our “hypercube scalar” follows directly from a very general prescription; no particular tuning for a good dispersion is involved. This raises hope that the same prescription is also successful for other quantities.

For comparison, we consider a Symanzik improved scalar by including additional couplings along the axes over two lattice spacings. The action

$$S[\phi] = \frac{1}{2} \sum_{x,y} \phi_x \left[ \delta_{x,y} \left( \frac{8d}{3} + m^2 \right) + \sum_{\mu} \left( -\frac{4}{3} \delta_{x+\hat{\mu},y} + \frac{1}{12} \delta_{x+2\hat{\mu},y} \right) \right] \phi_y \quad (3.1)$$

is  $O(a^2)$  improved; the remaining artifacts for the free scalars are of  $O(a^4)$ . The dispersion relation of this Symanzik improved scalar is also shown in Fig. 5 (left). By construction it is close to the continuum scalar for small momenta, but at  $k_1 = k_2 = 1.239$  it is hit by a higher branch, and the continuation of the curve is just the real part of two complex conjugate solutions, which are useless.

In exactly the same way one can improve the staggered fermions and arrives at the Naik fermion [27], which combines the discrete derivatives to nearest neighbors and over distances of three lattice spacings with the relative weights  $9/8$  and  $-1/24$ . A similar

construction starting from the Wilson fermion is called D234 action [28]. It turns out that its behavior is very similar to the one of the Symanzik improved scalar shown in Fig. 5 (left). Also Naik fermions and D234 fermions are hit by higher branches at  $|\vec{k}| = O(1)$ , which marks the end of the real solution for  $E(\vec{k})$ . Those dispersions are compared to the truncated perfect fermions in Ref. [10, 12].

Similarly, if we truncate an optimally local, perfect free gauge field to a 4d hypercube, we find an excellent (transverse) dispersion relation [12].

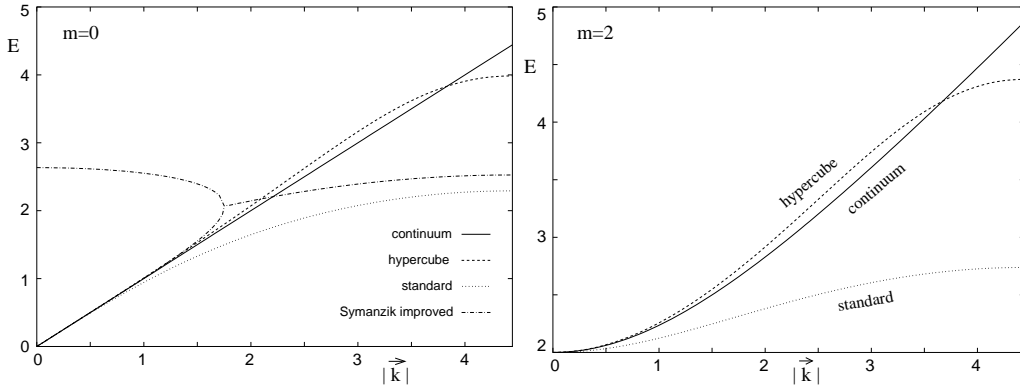


Figure 5: *The dispersion relation for a scalar of mass  $m = 0$  (left) and  $m = 2$  (right) in the (110) direction with the perfect, truncated perfect (“hypercubic”) and standard lattice action. For the hypercube action (as well as the standard action) there are no “ghosts” (higher branches) in any direction, in contrast to the Symanzik improved action.*

## 4 Thermodynamic properties

In thermodynamics the artifacts due finite lattice spacing are particularly bad [29], hence the use of improved actions is strongly motivated. Thermodynamics with quasi-perfect lattice actions has also been studied for pure  $SU(3)$  gauge theory [30], and for the 2d  $O(3)$  model [31].

First we consider massless scalars with  $N_t$  lattice points in the Euclidean time direction. We impose periodic boundary conditions in the 4 direction over those  $N_t$  lattice spacings. The pressure  $p$  on an infinite lattice with the standard action is given by [32]

$$\begin{aligned} \frac{p}{T^4} = & \frac{N_t^4}{(2\pi)^3} \int_{-\pi}^{\pi} d^3k \left[ \frac{1}{N_t} \sum_{n=1}^{N_t} \ln \Delta(\vec{k}, k_{4,n})^{-1} \Big|_{k_{4,n}=2\pi n/N_t} \right. \\ & \left. - \frac{1}{2\pi} \int_{-\pi}^{\pi} dk_4 \ln \Delta(\vec{k}, k_4)^{-1} \right], \end{aligned} \quad (4.1)$$

where  $T$  is the temperature.

To study the improvement of the lattice actions from Section 2 and 3, we just replace the standard lattice propagator in eq. (4.1) by the the fixed point or truncated fixed point

$r$	$m = 0$	$m = 1$	$m = 2$	$m = 4$
$d = 2$				
(00)	3.23975790	3.40289300	3.52616893	2.49915565
(10)	-0.61987895	-0.49256958	-0.26092482	-0.03241219
(11)	-0.19006053	-0.14542414	-0.06917628	-0.00607959
$d = 3$				
(000)	4.02729212	4.03823126	3.87615269	2.54721313
(100)	-0.39376711	-0.31766913	-0.17499188	-0.02402874
(110)	-0.11305592	-0.08745023	-0.04296647	-0.00419173
(111)	-0.03850230	-0.02898696	-0.01310490	-0.00094393
$d = 4$				
(0000)	4.54224606	4.45988071	4.11725747	2.58349386
(1000)	-0.25747697	-0.21082472	-0.12055239	-0.01814036
(1100)	-0.06814507	-0.05342220	-0.02721974	-0.00294419
(1110)	-0.02245542	-0.01701401	-0.00787336	-0.00062377
(1111)	-0.00802344	-0.00598647	-0.00261577	-0.00016008

Table 2: *The couplings  $\rho(r)$  of the truncated perfect scalar action in coordinate space for masses  $m = 0, 1, 2$  and  $4$ .*

propagator. In Fig. 6 the results for the three lattice actions are compared to the Stefan Boltzmann law in the continuum,

$$\frac{p}{T^4} = \frac{\pi^2}{90}. \quad (4.2)$$

In this respect even the “perfect actions” contain lattice artifacts. The reason is that we ignored “constant factors” when we performed the Gaussian functional integrals over  $\mathcal{D}\tilde{x}$  and  $\mathcal{D}\tilde{\sigma}$  in Section 2. For instance in the spectrum such factors have indeed no influence. However, they can depend on the temperature, yielding artifacts in thermodynamics. These artifacts are exponentially suppressed, and – as the Figures show – they disappear very fast as  $N_t$  increases. The truncation slows down a little the convergence to the Stefan Boltzmann value, but the behavior is still strongly improved compared to the standard lattice action. The latter suffers from quadratic artifacts (asymptotically  $0.38\pi^2/N_t^2$ ). Hypercubic truncation also yields quadratic artifacts, but only of about  $-0.05\pi^2/N_t^2$ .

As a second example, we return to  $T = 0$  but introduce a chemical potential  $\mu$  according to the instruction for general lattice actions given in Ref. [33]. We then measure the scaling ratio  $p/\mu^4$  for massless scalars. In the continuum it amounts to  $1/48\pi^2$ , and all lattice actions approach this value in the limit  $\mu \rightarrow 0$ . For finite  $\mu$  the lattice artifacts are visible. Fig. 6 (right) shows that they are dramatic for the standard action, whereas the artifacts in the hypercube action are again quite modest.

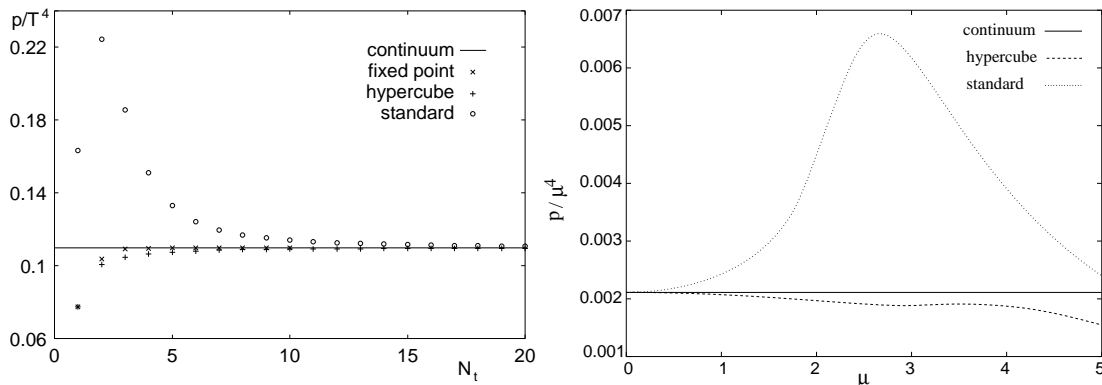


Figure 6: *Left: The ratio  $p/T^4$  at  $N_t$  discrete points in the Euclidean time direction for the perfect, the truncated perfect and the standard lattice action. Right: the scaling ratio  $p/\mu^4$  ( $\mu$ : chemical potential) at  $T = 0$  in the continuum, compared to different lattice actions.*

## 5 Preconditioning the hypercube scalar

If we want to simulate a hypercube scalar action, we are interested in efficient ways to compute the scalar determinant, analogous to the fermion determinant. There are a number of well established algorithms for this purpose, for an overview see Ref. [34]. The maximal speed of such methods is limited by the eigenvalue distribution. The goal of “preconditioning” is to transform the matrix such that its spectrum becomes more favorable with this respect. In particular, it is of advantage to squeeze the eigenvalues into a narrow interval.

In the case of the standard action we can order the matrix lines by passing successively through the even and the odd sub-lattice, and we obtain a matrix of the block form <sup>5</sup>

$$M = \begin{pmatrix} \mathbb{1} & -A \\ -A & \mathbb{1} \end{pmatrix}. \quad (5.1)$$

In a volume  $V$ ,  $M$  is a  $V \times V$  matrix which splits into 4 blocks of the same size ( $\mathbb{1}$  represents unity). We decompose  $M$  into  $M = \mathbb{1} - L - U$ , where  $L$ ,  $U$  are the strictly lower resp. upper triangular part of  $M$ . Now we define the matrices  $V_1 := \mathbb{1} - L$ ,  $V_2 := \mathbb{1} - U$ , which can be inverted trivially. The SSOR and the ILU preconditioning amount in this case both to the transformation

$$M' = V_1^{-1} M V_2^{-1} = \begin{pmatrix} \mathbb{1} & 0 \\ 0 & \mathbb{1} - A^2 \end{pmatrix}, \quad (5.2)$$

where  $\det M' = \det M$ . To solve a linear system of equations given by  $M$  we can now apply the Eisenstat trick [35], where we only need to invert triangular matrices. Moreover, referring to our criterion mentioned above, we can clearly expect the spectrum of  $M'$  to be closer to 1 than the spectrum of  $M$ .

<sup>5</sup>We re-scale the matrix such that the diagonal elements become 1.

For the hypercube scalar the situation is more complicated. To obtain a block structure in  $M$ , we have to decompose the lattice into  $2^d$  sub-lattices, which we go through successively. This sub-lattice structure is known from staggered fermions. We denote this extension of the “red-black” scheme as “*rainbow preconditioning*”. Thus we obtain  $2^d$  unit blocks along the diagonal of  $M$ , and many more nonzero elements than it is the case for the standard action. They arise from the  $d$  hopping parameters. We denote the maximal magnitude of the elements in  $L$  and  $U$  as  $O(\varepsilon)$ . We still apply the multiplication (5.2) and arrive at

$$M' = \mathbb{1} - \left( \sum_{i \geq 1}^V L^i \right) \left( \sum_{j \geq 1}^V U^j \right) = \mathbb{1} - LU - O(\varepsilon^3). \quad (5.3)$$

We cannot eliminate the off-diagonal elements to such a large extent as it was possible for the standard action, because there are more of them from the beginning. On the other hand, we can still expect the spectrum of  $M'$  to be much closer to 1, typically the eigenvalues are  $1 - O(\varepsilon^2)$ . Since  $\varepsilon$  is clearly suppressed for the hypercube scalar – compared to the  $\varepsilon$  occurring in the standard action – the suppression of the deviation from the unit matrix ( $O(\varepsilon)$  for  $M$ ,  $O(\varepsilon^2)$  for  $M'$ ) becomes even more powerful. In addition we are still in agreement with the conditions for the Eisenstat trick.

To observe this effect, we consider the 2d case for  $m = 1$ , where the off-diagonal elements are 0,  $-0.072375$  or  $-0.0213675$ , as we know from Table 2. On a  $6 \times 6$  lattice one obtains the spectrum illustrate in Fig. 7 for  $M$  (left), and for  $M'$  (right). The height of the lines represents the algebraic multiplicity of the corresponding eigenvalues. We see that the eigenvalues of  $M'$  are indeed concentrated close to 1, and all of them are  $\leq 1$ , as one may suspect from eq. (5.3). In particular, the eigenvalue most distant from 1 is 0.72185 for  $M$ , and it moves to 0.94060 for  $M'$ . Note also that  $M$  does not have an eigenvalue 1, but in  $M'$  there are 18 of them (plus 2 at 0.99537, which are hidden in Fig. 7). The “squeezing” effect is indeed stronger for the truncated perfect action than for the standard action.

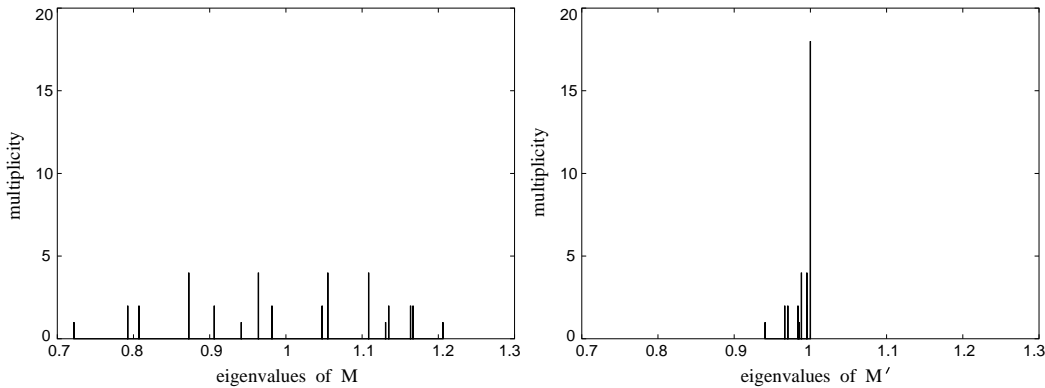


Figure 7: The eigenvalue distribution of the hypercube scalar matrix  $M$  – before preconditioning – (left), and of the corresponding matrix  $M'$  – after preconditioning – (right) on a  $6 \times 6$  lattice.



We conclude that preconditioning is still applicable and efficient for hypercube actions. The same holds for hypercube fermions (perfect fermions truncated to a unit hypercube); for first experiments in QCD, see Ref. [26].

## 6 Non hypercubic lattices

### 6.1 Anisotropic lattices

It is straightforward to write down the perfect free scalar propagator on arbitrary hyper-rectangular lattices. We call the lattice spacing in  $\mu$  direction  $a_\mu$ ,  $\mu = 1, \dots, d$ . Then the blocking from the continuum involves an integral over the hyper-rectangular lattice cells. The smearing parameter  $\alpha$  is also affected, since it has dimension  $mass^{-2}$ . We have to make a choice, for which 1d projection we want to obtain ultralocality. If this is the case for the mapping on the  $\nu$  axis, then the generalized perfect propagator reads

$$\begin{aligned} G_{ani}(k) &= \sum_{l \in \mathbb{Z}^d} \Delta(k + 2\pi(l/a)) \Pi^2(k + 2\pi(l/a)) + \frac{\bar{\alpha}}{a_\nu^2} \\ (l/a) &:= (l_1/a_1, \dots, l_d/a_d) \\ \Pi(k) &= \prod_{\mu=1}^d \frac{\hat{k}_\mu}{k_\mu}, \quad \hat{k}_\mu := \frac{2}{a_\mu} \sin \frac{k_\mu a_\mu}{2}, \end{aligned} \tag{6.1}$$

where  $k \in B = ] - \pi/a_1, \pi/a_1] \times \dots \times ] - \pi/a_d, \pi/a_d]$ , and  $\bar{\alpha}$  is still the mass dependent smearing parameter from eq. (2.17). Note that the Poincaré invariance of the spectrum persists, whatever the lattice spacings.

Anisotropic lattices are often used in thermodynamics. To simulate at finite temperature on isotropic lattices, there are typically just  $N_t = 4$  to 8 points available in the Euclidean time direction. In order to measure correlators precisely one would like to have a larger  $N_t$ . The anisotropy permits to invest a larger fraction of the available lattice points in the 4 direction (in a hypercubic volume). One introduces a spatial lattice constant  $a_\sigma$ , and a temporal one  $a_t < a_\sigma$ .

If one then measures masses in all directions, one recovers isotropy up to lattice artifacts, which can be used as a test of improved actions in this context. If the improvement is successful, one may use a coarse spatial lattice, but a small  $a_t$ . The dispersion relations are the same as on the hypercubic lattice, up to a rescaling of the axes. Hence the strong improvement that we observed for the (truncated) perfect scalars persists.

In improved actions, the presence of “ghosts” (higher branches in the dispersion relation) can cause some trouble because they distort the Hermiticity of the transfer matrix. In the fully perfect action there are necessarily an infinite number of such ghosts – corresponding to the sum over  $l$ . In Symanzik improved actions there are usually a few ghosts, and by some modifications it is possible to get rid of some of them or all of them, if one takes in account other disadvantages (for “D234 fermions” this has been discussed in Ref.

[28]). The hypercube scalars – as well as all hyper-rectangular scalars – have the virtue that they are free of ghosts to start with, cf. Fig. 5.

## 6.2 Triangular lattices

By blocking from the continuum we can also derive efficiently perfect actions on triangular lattices or honey comb lattices. Such actions are completely unexplored so far. As an illustration we consider the case of a 2d lattice built from regular triangles with lattice spacing 1. Here the blocking from the continuum involves integrals over the hexagonal lattice cells, which form the dual lattice.<sup>6</sup> In coordinates of the suitable axes – with an angle of  $\pi/3$  – we find that the  $\Pi$  function introduced in Section 2 is replaced by

$$\Pi_{tria}(k) = \frac{8}{3k_1k_2(k_1+k_2)} \left[ k_1 \cos \frac{k_1}{2} + k_2 \cos \frac{k_2}{2} - (k_1+k_2) \cos \frac{k_1+k_2}{2} \right]. \quad (6.2)$$

We recognize the exchange symmetry of the axes and the special rôle of the edges of the triangular Brillouin zone. Like the hypercubic  $\Pi$  function, also  $\Pi_{tria}$  only contains removable singularities, and in the limit  $k_1, k_2 \rightarrow 0$  it becomes 1, which confirms the normalization.

If we only let  $k_2 \rightarrow 0$ , we arrive at

$$\Pi_{tria}(k_1, 0) = \frac{8}{3k_1^2} \left[ 1 - \cos \frac{k_1}{2} + \frac{k_1}{2} \sin \frac{k_1}{2} \right]. \quad (6.3)$$

Remarkably, this is different from  $\Pi(k_1)$ .

The blocking constraint

$$\phi_x = \int_{H_x} d^2y \, \varphi(y) \quad (6.4)$$

–  $H_x$  being the hexagon with unit diameter and center  $x$  – takes in momentum space the form

$$\begin{aligned} \phi(k) &= \frac{3}{4} \sum_{l \in \mathbb{Z}^2} \varphi(k_l) \Pi_{tria}(k_l), \\ k_l &:= k + \frac{4\pi}{3} \begin{pmatrix} 2 & -1 \\ -1 & 2 \end{pmatrix} l := k + \frac{4\pi}{3} l'. \end{aligned} \quad (6.5)$$

Note that  $l'$  does not extend over  $\mathbb{Z}^2$ ; it only covers the points where  $l'_1 - l'_2$  is an integer multiple of 3. These points build again a triangular lattice. They are the centers of the Brillouin zones, which have a hexagonal form. The lattice momentum  $k$  in eq. (6.5) is in the Brillouin zone around zero, namely the hexagon with the corners  $(\pm 4\pi/3, 0)$ ,  $(0, \pm 4\pi/3)$ ,  $(4\pi/3, -4\pi/3)$  and  $(-4\pi/3, 4\pi/3)$ . Thus the integral over  $k$ , together with the

---

<sup>6</sup>For the perfect action on a honey comb lattice it is the other way round, the cells to be integrated over are triangles in two different orientations.

sum over  $l'$ , just covers the continuum momentum space. Note that this structure agrees with that fact that a plane wave along one axis may have momentum  $4\pi$  before being caught in periodicity.

Considering that the scalar product is transformed in this coordinate system, we arrive at the perfect triangular propagator

$$G_{tria}(k) = \sum_{l \in \mathbb{Z}^2} \frac{\Pi_{tria}^2(k_l)}{k_{l,1}^2 + k_{l,2}^2 + k_{l,1}k_{l,2} + m^2} + \alpha . \quad (6.6)$$

The further steps – evaluation of the inverse propagator in coordinate space, truncation etc. – are straightforward, in analogy to Sections 2 to 4.

## 7 B-spline blocking

We return to the hypercubic lattice and we want to explore some new versions of the blocking from the continuum. The hope is to find convolution functions, which have advantages over the simple prescription described in Section 2, particularly in view of locality.

First we introduce the wavelet or B spline language [36] in  $d = 1$ , in a dialect which is suitable for our purposes. The zeroth B spline function is just a  $\delta$  function,

$$f_0(x) = \delta(x). \quad (7.1)$$

Inductively we proceed from order  $N$  to  $N + 1$  as follows:

$$f_{N+1}(x) = \int_{-\infty}^x dy \left[ f_N(y + \frac{1}{2}) - f_N(y - \frac{1}{2}) \right] = \int_{x-1/2}^{x+1/2} f_N(y) dy. \quad (7.2)$$

This implies for instance

$$\begin{aligned} f_1(x) &= \begin{cases} 1 & |x| < \frac{1}{2} \\ 0 & \text{otherwise} \end{cases}, & f_2(x) &= \begin{cases} 1 - |x| & |x| < 1 \\ 0 & \text{otherwise} \end{cases} \\ f_3(x) &= \begin{cases} \frac{3}{4} - x^2 & |x| < \frac{1}{2} \\ \frac{1}{2}(\frac{3}{2} - |x|)^2 & \frac{1}{2} \leq |x| < \frac{3}{2} \\ 0 & \text{otherwise} \end{cases}, & \text{etc.} \end{aligned} \quad (7.3)$$

We note a few properties:  $f_N(x) = f_N(-x)$ ,  $f_N(\pm\infty) = 0$ ,  $f_N(x) \geq 0$ ,  $\int_{-\infty}^{\infty} f_N(x) dx = 1$ ,  $f_N(x)$  is maximal in  $x = 0$  and consists of monomial pieces of order  $N$ . Furthermore we observe

$$\sum_{j \in \mathbb{Z}} f_N(x + j) \equiv 1 \quad (\text{for all } x, N \geq 1). \quad (7.4)$$

For the periodic blocking from the continuum on a unit lattice, the means that all continuum points contribute with the same weight to the lattice variables (“democracy among the continuum points”).

For increasing  $N$  the functions seem flatter and smoother (although  $f_3$  is still not continuously differentiable). The support ranges from  $-N/2$  to  $N/2$ .

In  $d$  dimensions we simply define  $f_N(x) = \prod_{\mu=1}^d f_N(x_\mu)$ . If we use  $f_N(x)$  as the convolution function for blocking matter fields from the continuum, then it is sensible to insert

$$f_{N,\mu} := f_{N+1}(x_\mu) \prod_{\nu \neq \mu} f_N(x_\nu) \quad (7.5)$$

for the non-compact Abelian gauge field  $A_\mu$ . This just provides the connection of nearest neighbor lattice matter field variables, i.e. we integrate over all the straight continuum connections of corresponding points in adjacent lattice cells. This generalizes the prescription applied in Ref. [11].

The simplest approach in this framework is the decimation RGT (in coordinate space), which defines the lattice variables as

$$\phi_x = \int d^d y f_0(x-y) \varphi(y), \quad x \in \mathbb{Z}^d. \quad (7.6)$$

However, the corresponding expression for the free propagator in momentum space,

$$G_0(k) = \sum_{l \in \mathbb{Z}^d} \frac{1}{(k + 2\pi l)^2 + m^2} + \alpha \quad (7.7)$$

only converges in  $d = 1$ . Still the blocking scheme which arises for gauge fields in this approach occurs in the literature [37]. On the other hand, for all  $N \geq 1$  the convergence of the sum in the propagator is guaranteed, both, for  $f_N$  and for  $f_{N,\mu}$ .

What has been done so far in this paper, and in Refs. [4, 11], is one step forward to the use of  $f_1$  for the matter fields (see eq. (2.11)), and  $f_{1,\mu}$  for the gauge fields. This already provides a promising degree of locality.

To explore further possibilities, the obvious next step is to consider higher orders in this pattern,

$$\phi_x = \int d^d y \left[ \prod_{\nu=1}^d f_N(x_\nu - y_\nu) \right] \varphi(y). \quad (7.8)$$

In momentum space we find inductively

$$f_N(k) = \prod_{\mu=1}^d \left( \frac{\hat{k}_\mu}{k_\mu} \right)^N, \quad (7.9)$$

and the perfect scalar propagator takes the form

$$G_N(k) = \sum_{l \in \mathbb{Z}^d} \frac{\Pi^{2N}(k + 2\pi l)}{(k + 2\pi l)^2 + m^2} + \alpha_N. \quad (7.10)$$

decay coefficient	$f_1$	$f_2$	$F_2$
$c_1$	3.805	2.996	3.348
$c_2/\sqrt{2}$	3.876	3.159	3.566
$c_3/\sqrt{3}$	3.397	3.156	3.757
$c_4/2$	3.258	3.179	3.333

Table 3: *The competition for locality: we give the coefficients of the exponential decay,  $|\rho(i, 0, 0, 0)| \propto \exp\{-c_1 i\}, \dots, |\rho(i, i, i, i)| \propto \exp\{-c_4 i\}$ , fitted in the interval  $i = 1 \dots 5$ . The decay coefficients  $c_i$  are divided by  $\sqrt{i}$ , so that the level of rotation invariance is revealed too. In that respect, the use of  $F_2$ , and especially  $f_2$ , is even better than the standard blocking function  $f_1$  (piece-wise constant).*

For increasing  $N$  the peak of  $f_N(k)$  around  $k = 0$  becomes steeper, in agreement with the observation that  $f_N(x)$  turns less localized. Still the 1d propagator can be made ultralocal for any order  $N$ , if we choose the suitable smearing parameter  $\alpha_N$ . The first few orders require at  $m = 0$

$$\alpha_0 = 0, \quad \alpha_1 = \frac{1}{6}, \quad \alpha_2 = \frac{1}{4} - \frac{\hat{k}^2}{120}, \quad \alpha_3 = \frac{1}{3} - \frac{\hat{k}^2}{40} + \frac{\hat{k}^4}{5040} \quad \text{etc.} \quad (7.11)$$

The general form is a polynomial in  $\hat{k}^2$  of order  $N - 1$ .

The use of these B-spline functions as they stand makes the action less local for  $N$  increasing beyond 1, so that we cannot find anything better than  $N = 1$  (the case we had before) within this scheme. The case  $N = 2$  is not that bad, but beyond the level of locality decreases rapidly. This suggests that a strong overlap of the blocking functions for different sites is unfavorable for locality, which was also confirmed by considering other types of functions.

However, we may squeeze the functions again into the interval  $[-1/2, 1/2]$  on each axis by just rescaling  $x$  and correcting the normalization,  $F_N(x) = N f_N(Nx)$ . Thus we give up the property (7.4). Instead of a democratic treatment of the continuum points we do something between that and decimation. It turns out that now the locality is in business, at least for

$$F_2(x) = 2(1 - 2|x|) \Theta(1/2 - |x|). \quad (7.12)$$

We summarize these observations in Table 3. We recommend to focus on  $N = 2$ , and we denote the corresponding blocking function  $F_2$  as “*Eiffel tower function*”. It has the virtue that it can be related to a relatively simple blocking from a fine to a coarse lattice, such that we reproduce the same fixed point. If  $N$  increases, it becomes more and more difficult to establish such relations; the cells, where the block variables are build, have to be larger and larger. However, this property is needed if we ultimately want to combine the blocking from the continuum with a subsequent multigrid minimization. Moreover, the step beyond  $N = 2$  is not profitable in view of locality.

$\rho(0000)$	$\rho(1000)$	$\rho(1100)$	$\rho(1110)$	$\rho(1111)$
4.09671070	-0.23791704	-0.056450784	-0.021127525	-0.010154672

Table 4: *The couplings  $\rho(r)$  of the truncated perfect scalar at  $m = 0$ , constructed from the “Eiffel tower” blocking.*

We truncate the FPA obtained from blocking with the Eiffel tower function  $F_2$  again to a unit hypercube. The couplings of this new hypercube scalar are given in Table 4. Its properties regarding the spectrum and thermodynamics are on the same level as the hypercube scalar obtained from the standard approach and given in Table 2; all in all the hypercube scalar of Section 3 is slightly superior, but in specific respects the Eiffel tower hypercube scalar is better.

For the Wilson-like fermions we observed a qualitatively similar behavior; in that case the Eiffel tower blocking looks even a little better than the blocking with the usual step function, see Appendix B.

## 8 Conclusions and outlook

We have constructed perfect lattice formulations for free scalar fields of any mass, and we optimized their locality. We also explored new aspects of the RGT improvement technique, in particular regarding non-hypercubic lattices and blocking functions, which are not piece-wise constant. We then truncated the couplings of a perfect scalar to a short range – so that the formulation become applicable in simulations – and showed that a drastic improvement persists. This was observed from the dispersion relation as well as thermodynamic properties. In view of the numerical treatment we showed that a new variant of preconditioning is applicable and powerful, which is also true for truncated perfect fermions.

Simulations of truncated perfect scalars have been performed in  $d = 1$  for the anharmonic oscillator [14]. The 2d truncated perfect scalars of Section 3 have been used by W. Loinaz in an ongoing numerical study of the critical coupling in the  $\lambda\phi^4$  model, along the lines of Ref. [38]. Improved scalar actions play a rôle in bosonic spin models, in particular the non-linear  $\sigma$ -model [15, 21, 39]. A potential field of application in  $d = 4$  is the Higgs model (for a very recent application of Symanzik improvement, see Ref. [40]). Finally the truncated perfect Laplacian could be applied also for an improved gauge fixing in the spirit of Ref. [41].

**Acknowledgment** *I would like to thank Ph. de Forcrand for encouraging me to finish this paper, a draft of which has been around for more than two years. The first part is based on techniques worked out in collaboration with R. Brower, S. Chandrasekharan and in particular U.-J. Wiese.*

## A The perfect propagator under a RGT

We want to demonstrate the perfectness of the propagator  $G(k)$  in eq. (2.14) by explicitly applying a block factor  $n$  RGT. The perfect action is supposed to reproduce itself, up to a rescaling of the mass.

From Ref. [2] we can extract the general recursion relation for the propagator under a block factor  $n$  RGT (the  $n \rightarrow \infty$  limit of which is given in eq. (2.9)),

$$G'(k)|_m = \frac{1}{n^2} \sum_{\bar{l}} G((k + 2\pi\bar{l})/n)|_m \prod_{\mu=1}^d \left( \frac{\sin(k_\mu/2)}{n \sin((k_\mu + 2\pi\bar{l}_\mu)/2n)} \right)^2 + \alpha_n, \quad (\text{A.1})$$

where  $\bar{l} \in \{0, 1, 2, \dots, n-1\}^d$ . Inserting now the perfect propagator of eq. (2.14) at mass  $m$  we obtain

$$\begin{aligned} G'(k)|_m &= \frac{1}{n^2} \sum_{\bar{l}} \left[ \frac{\alpha_n}{1 - 1/n^2} \prod_{\mu} \left( \frac{\sin(k_\mu/2)}{n \sin((k_\mu + 2\pi\bar{l}_\mu)/2n)} \right)^2 + \right. \\ &\quad \left. \sum_{l \in \mathbb{Z}^d} \frac{1}{(k + 2\pi\bar{l} + 2\pi nl)^2/n^2 + m^2} \times \right. \\ &\quad \left. \prod_{\mu} \left( \frac{2 \sin((k_\mu + 2\pi\bar{l}_\mu)/2n)}{(k_\mu + 2\pi\bar{l}_\mu + 2\pi nl_\mu)/n} \frac{\sin(k_\mu/2)}{n \sin((k_\mu + 2\pi\bar{l}_\mu)/2n)} \right)^2 \right] + \alpha_n \\ &= \alpha_n \left[ 1 + \frac{1}{(n^2 - 1)n^{2d}} \sum_{\bar{l}} \prod_{\mu} \left( \frac{\sin(k_\mu/2)}{\sin((k_\mu + 2\pi\bar{l}_\mu)/2n)} \right)^2 \right] + \\ &\quad \sum_{\bar{l}} \sum_{l \in \mathbb{Z}^d} \frac{1}{(k + 2\pi[\bar{l} + nl])^2 + (nm)^2} \Pi(k + 2\pi[\bar{l} + nl])^2 \\ &= G(k)|_{nm} \end{aligned} \quad (\text{A.2})$$

This is the desired result, confirming the claims of Section 2. In the last step we have used the identity

$$\sum_{j=0}^{n-1} \left( \frac{\sin(x/2)}{\sin((x + 2\pi j)/2n)} \right)^2 \equiv n^2.$$

Amazingly, I could not find this – or a directly related – identity in any table of formulae. It can be demonstrated, however, by inserting

$$\frac{\sin(ny/2)}{\sin(y/2)} \equiv \sum_{k=-(n-1)/2}^{(n-1)/2} \exp(iky)$$

(for odd  $n$  the sum runs over half integers) and then summing over  $j$ .

$y - x$	$\rho_1(y - x)$	$\lambda(y - x)$
(0, 0, 0, 0)	0	1.83043692
(1, 0, 0, 0)	0.158134654	-0.0577452799
(1, 1, 0, 0)	0.0290077129	-0.0295719810
(1, 1, 1, 0)	0.0108088580	-0.0161376837
(1, 1, 1, 1)	0.00476409657	-0.00889632880

Table 5: *The couplings of the massless hypercube fermion constructed by using the Eiffel tower function  $F_2$  as RGT blocking function, and by truncating the FPA.*

## B Eiffel tower blocking for fermions

It is straightforward to extend the considerations for non hypercubic lattices and non piece-wise constant blocking functions (Sections 6 and 7) to fermions. The most promising variant for applications is the Eiffel tower blocking, so we add in this appendix the corresponding results for Wilson-type fermions. We denote the lattice Dirac operator as  $D = \rho_\mu \gamma_\mu + \lambda$ , where  $\rho_\mu$  is odd in  $\mu$  direction and even otherwise, while the Dirac scalar  $\lambda$  is entirely even. The prefect free propagator obtained from Eiffel tower blocking – i.e. using the blocking function  $F_2$  given in eq. (7.12) – reads

$$D^{-1}(k) = \sum_{l \in \mathbb{Z}^d} \frac{1}{i(\vec{k} + 2\pi\vec{l}) + m} \prod_{\mu=1}^d \left( \frac{8[1 - \cos((k_\mu + 2\pi l_\mu)/2)]}{(k_\mu + 2\pi l_\mu)^2} \right)^2 + \alpha_f. \quad (\text{B.1})$$

For massless fermions, 1d ultralocality is provided by the RGT smearing parameter  $\alpha_f = 1/2$  (this is exactly the same value which is also required for the piece-wise constant blocking function  $f_1 = F_1$  [11]). Here even  $F_{N>2}$  yields comparable locality of  $D$ , but for reasons pointed out in Section 7 we prefer to stay with  $F_2$ . There the locality of the FPA is slightly better than for  $f_1$ : using  $F_2$ , the decay along the 4d diagonal has the exponential coefficients (analogous to  $c_4$  in Section 2) 5.037 (for  $\rho_\mu$ ) and 5.109 (for  $\lambda$ ), to be compared with 4.931 (for  $\rho_\mu$ ) and 5.039 (for  $\lambda$ ) when we use  $f_1$ . Therefore truncation yields a hypercube fermion, which is at least of the same quality as the one presented in Ref. [12]; its dispersion relation does not start with an overshoot, it is excellent up to  $|\vec{k}| \approx 2$ , and also other properties are in business. The new hypercube fermion couplings are given in Table 5.

## References

- [1] K. Wilson and J. Kogut, Phys. Rep. C12 (1974) 75.  
K. Wilson, Rev. Mod. Phys. 47 (1975) 773.
- [2] T. Bell and K. Wilson, Phys. Rev. B11 (1975) 3431.



- [3] K. Wilson, in *New Pathways in High Energy Physics II*, ed. A. Perlmutter (Plenum, New York, 1976) 243.
- [4] W. Bietenholz and U.-J. Wiese, Phys. Lett. B378 (1996) 222.
- [5] S. Cronjäger, Blockspintransformationen für freie Fermionen, diploma thesis, Hamburg University (1985).
- [6] U.-J. Wiese, Phys. Lett. B315 (1993) 417.
- [7] G. Mai, Ein Blockspin für  $2^{d/2}$  Fermionen, diploma thesis, Hamburg University (1989).
- [8] W. Bietenholz and U.-J. Wiese, Nucl. Phys. B (Proc. Suppl.) 34 (1994) 516.
- [9] H. Dilger, Nucl. Phys. B490 (1997) 331.
- [10] W. Bietenholz, R. Brower, S. Chandrasekharan and U.-J. Wiese, Nucl. Phys. B 495 (1997) 285.
- [11] W. Bietenholz and U.-J. Wiese, Nucl. Phys. B464 (1996) 319.
- [12] W. Bietenholz, R. Brower, S. Chandrasekharan and U.-J. Wiese, Nucl. Phys. B (Proc. Suppl.) 53 (1997) 921.
- [13] K. Orginos et al., Nucl. Phys. B (Proc. Suppl.) 60 A-C (1998) 904.
- [14] W. Bietenholz and T. Struckmann, Int. J. Mod. Phys. C10 (1999) 531.
- [15] P. Hasenfratz and F. Niedermayer, Nucl. Phys. B414 (1994) 785.
- [16] M. Griessl, G. Mack, G. Palma and Y. Xylander, Nucl. Phys. B477 (1996) 878.  
T. Takaishi and Ph. de Forcrand, Phys. Lett. B428 (1998) 157.  
Ph. de Forcrand et al., hep-lat/9806008.
- [17] T. DeGrand, A. Hasenfratz, P. Hasenfratz and F. Niedermayer, Nucl. Phys. B454 (1995) 587, 615.  
M. Blatter and F. Niedermayer, Nucl. Phys. B482 (1996) 286.  
T. Bhattacharya, R. Gupta and W. Lee, hep-lat/9910046.
- [18] W. Bietenholz, Nucl. Phys. B (Proc. Suppl.) 60A-C (1998) 955.
- [19] L. Kadanoff and A. Houghton, Phys. Rev. B11 (1975) 377.
- [20] J. Hirsch and S. Shenker, Phys. Rev. B27 (1983) 1736.
- [21] A. Tsapalis and U.-J. Wiese, Nucl. Phys. B (Proc. Suppl.) 53 (1997) 948.
- [22] W. Bietenholz, E. Focht and U.-J. Wiese, Nucl. Phys. B436 (1995) 385.

- [23] P. Ginsparg and K. Wilson, Phys. Rev. D25 (1982) 2649.
- [24] W. Bietenholz and U.-J. Wiese, Nucl. Phys. B (Proc. Suppl.) 47 (1996) 575.
- [25] T. DeGrand, Phys. Rev. D58 (1998) 094503; hep-lat/9903006.
- [26] W. Bietenholz, N. Eicker, A. Frommer, Th. Lippert, B. Medeke, K. Schilling and G. Weuffen, Comput. Phys. Commun. 119 (1999) 1.
- [27] S. Naik, Nucl. Phys. B316 (1989) 238.
- [28] M. Alford, T. Klassen and G.P. Lepage, Nucl. Phys. B496 (1997) 377.
- [29] F. Niedermayer, Nucl. Phys. B (Proc. Suppl.) 53 (1997) 56.
- [30] A. Papa, Nucl. Phys. B478 (1996) 335.
- [31] S. Spiegel, Phys. Lett. B400 (1997) 352.
- [32] J. Engels, F. Karsch and H. Satz, Nucl. Phys. B205 [FS5] (1982) 239.
- [33] W. Bietenholz and U.-J. Wiese, Phys. Lett. B426 (1998) 114.  
W. Bietenholz, Nucl. Phys. A642 (1998) 537.
- [34] A. Frommer, Nucl. Phys. B (Proc. Suppl.) 53 (1997) 120.
- [35] S. Eisenstat, SIAM J. Sc. Stat. Comput. 2 (1981) 1.
- [36] Generalities can be found for instance in  
C. Chui, *An Introduction to Wavelets*, Academic Press, Boston 1992.  
G. Kaiser, *A Friendly Guide to Wavelets*, Birkhäuser, Boston 1994.  
For an earlier suggestion to use the wavelet formalism in the block variable RGT, see  
G. Battle, in *Wavelets - A Tutorial in Theory and Applications*, C. Chui ed., Academic Press, San Diego 1992, p. 73.  
A related new approach was presented recently in  
C. Best, hep-lat/9909151.
- [37] J. Hetrick, Nucl. Phys. B (Proc. Suppl.) 47 (1996) 823.
- [38] W. Loinaz and R. Willey, Phys. Rev. D58 (1998) 076003.
- [39] A. Gottlob, M. Hasenbusch and K. Pinn, Phys. Rev. D54 (1996) 1736.  
S. Caracciolo, A. Montanari and A. Pelissetto, Nucl. Phys. B556 (1999) 295.  
M. Bartels, G. Mack and G. Palma, hep-lat/9909149.
- [40] P. Dimopoulos, K. Farakos and G. Koutsoumbas, hep-lat/9911012.
- [41] F. Bonnet, P. Bowman, D. Leinweber, D. Richards and A. Williams, hep-lat/9909110.  
Ph. de Forcrand et al., in preparation.